Sub-μm^2 power splitters by using silicon hybrid plasmonic waveguides

Article *in* Optics Express · January 2011

DOI: 10.1364/OE.19.000838 · Source: PubMed

Sub-μm^2 power splitters by using silicon hybrid plasmonic waveguides

Jianwei Wang,[1] Xiaowei Guan,[1] Yingran He,[1] Yaocheng Shi,[1,2] Zhechao Wang,[1,2] Sailing He,[1,2] Petter Holmström,[2,3] Lech Wosinski,[2,3] Lars Thylen,[2,3] and Daoxin Dai[1,2*]

[1]*Centre for Optical and Electromagnetic Research, State Key Laboratory for Modern Optical Instrumentation, Zhejiang University, East Building No.5, Zijingang Campus, Zhejiang University, Hangzhou 310058, China*
[2]*JORCEP (Joint Research Center of Photonics of the Royal Institute of Technology (KTH) and Zhejiang University), Zhejiang University, Hangzhou 310058, China*
[3]*Laboratory of Photonics and Microwave Engineering, Royal Institute of Technology (KTH), 16440 Kista, Sweden.*
** dxdai@zju.edu.cn*

Abstract: Nano-scale power splitters based on Si hybrid plasmonic waveguides are designed by utilizing the multimode interference (MMI) effect as well as Y-branch structure. A three-dimensional finite-difference time-domain method is used for simulating the light propagation and optimizing the structural parameters. The designed 1×2 50:50 MMI power splitter has a nano-scale size of only 650 nm×530 nm. The designed Y-branch power splitter is also very small, i.e., about 900 nm×600 nm. The fabrication tolerance is also analyzed and it is shown that the tolerance of the waveguide width is much larger than±50 nm. The power splitter has a very broad band of over 500 nm. In order to achieve a variable power splitting ratio, a 2×2 two-mode interference coupler and an asymmetric Y-branch are used and the corresponding power splitting ratio can be tuned in the range of 97.1%:2.9%-1.7%:98.3% and 84%:16%-16%:84%, respectively. Finally a 1×4 power splitter with a device footprint of 1.9 μm×2.6 μm is also presented using cascaded Y-branches.

OCIS codes: (240.6680) Surface plasmons; (250.5300) Photonic integrated circuits; (130.1750) Components.

References and links

1. T. Goto, Y. Katagiri, H. Fukuda, H. Shinojima, Y. Nakano, I. Kobayashi, and Y. Mitsuoka, "Propagation loss measurement for surface plasmon-polariton modes at metal waveguides on semiconductor substrates," Appl. Phys. Lett. **84**(6), 852–854 (2004).
2. R. Zia, M. D. Selker, P. B. Catrysse, and M. L. Brongersma, "Geometries and materials for subwavelength surface plasmon modes," J. Opt. Soc. Am. A **21**(12), 2442–2446 (2004).
3. B. Wang, and G. P. Wang, "Surface plasmon polariton propagation in nanoscale metal gap waveguides," Opt. Lett. **29**(17), 1992–1994 (2004).
4. K. Tanaka, M. Tanaka, and T. Sugiyama, "Simulation of practical nanometric optical circuits based on surface plasmon polariton gap waveguides," Opt. Express **13**(1), 256–266 (2005).
5. F. Kusunoki, T. Yotsuya, J. Takahara, and T. Kobayashi, "Propagation properties of guided waves in index guided two-dimensional optical waveguides," Appl. Phys. Lett. **86**(21), 211101 (2005).
6. D. F. P. Pile, and D. K. Gramotnev, "Channel plasmon-polariton in a triangular groove on a metal surface," Opt. Lett. **29**(10), 1069–1071 (2004).
7. S. I. Bozhevolnyi, V. S. Volkov, E. Devaux, J. Y. Laluet, and T. W. Ebbesen, "Channel plasmon subwavelength waveguide components including interferometers and ring resonators," Nature **440**(7083), 508–511 (2006).
8. L. Liu, Z. H. Han, and S. L. He, "Novel surface plasmon waveguide for high integration," Opt. Express **13**(17), 6645–6650 (2005).
9. G. Veronis, and S. H. Fan, "Bends and splitters in metal-dielectric-metal subwavelength plasmonic waveguides," Appl. Phys. Lett. **87**(13), 131102 (2005).
10. E. Ozbay, "Plasmonics: merging photonics and electronics at nanoscale dimensions," Science **311**(5758), 189–193 (2006).
11. R. F. Oulton, V. J. Sorger, D. A. Genov, D. F. P. Pile, and X. Zhang, "A hybrid plasmonic waveguide for subwavelength confinement and long-range propagation," Nat. Photonics **2**(8), 496–500 (2008).
12. D. Dai, and S. He, "A silicon-based hybrid plasmonic waveguide with a metal cap for a nano-scale light confinement," Opt. Express **17**(19), 16646–16653 (2009).

#137029 - $15.00 USD Received 22 Oct 2010; revised 24 Nov 2010; accepted 21 Dec 2010; published 6 Jan 2011

13. D. Dai, and S. He, "Low-loss hybrid plasmonic waveguide with double low-index nano-slots," Opt. Express **18**(17), 17958–17966 (2010).
14. R. F. Oulton, V. J. Sorger, T. Zentgraf, R. M. Ma, C. Gladden, L. Dai, G. Bartal, and X. Zhang, "Plasmon lasers at deep subwavelength scale," Nature **461**(7264), 629–632 (2009).
15. D. X. Dai, L. Yang, and S. L. He, "Ultrasmall thermally tunable microring resonator with a submicrometer heater on Si nanowires," J. Lightwave Technol. **26**(6), 704–709 (2008).
16. D. Dai, Y. Shi, and S. He, "Comparative study of the integration density for passive linear planar light-wave circuits based on three different kinds of nanophotonic waveguide," Appl. Opt. **46**(7), 1126–1131 (2007).
17. M. Fujii, J. Leuthold, and W. Freude, "Dispersion relation and loss of subwavelength confined mode of metal-dielectric-gap optical waveguides," IEEE Photon. Technol. Lett. **21**(6), 362–364 (2009).
18. M. Z. Alam, J. Meier, J. S. Aitchison, and M. Mojahedi, "Propagation characteristics of hybrid modes supported by metal-low-high index waveguides and bends," Opt. Express **18**(12), 12971–12979 (2010).
19. M. Wu, Z. Han, and V. Van, "Conductor-gap-silicon plasmonic waveguides and passive components at subwavelength scale," Opt. Express **18**(11), 11728–11736 (2010).
20. Y. Song, J. Wang, Q. Li, M. Yan, and M. Qiu, "Broadband coupler between silicon waveguide and hybrid plasmonic waveguide," Opt. Express **18**(12), 13173–13179 (2010).
21. L. Soldano, and E. Pennings, "Optical multi-mode interference devices based on self-imaging: principles and application," J. Lightwave Technol. **13**(4), 615–627 (1995).
22. Z. Han, and S. He, "Multimode interference effect in plasmonic subwavelength waveguides and an ultra-compact power splitter," Opt. Commun. **278**(1), 199–203 (2007).
23. B.-K. Yang, S.-Y. Shin, and D. Zhang, "Ultrashort polarization splitter using two-mode interference in silicon photonic wires," IEEE Photon. Technol. Lett. **21**(7), 432–434 (2009).
24. S. Suzuki, T. Kitoh, Y. Inoue, Y. Yamada, Y. Hibino, K. Moriwaki, and M. Yanagisawa, "Integrated optic Y-branching waveguides with an asymmetric branching ratio," Electron. Lett. **32**(8), 735–736 (1996).
25. S. H. Tao, Q. Fang, J. F. Song, M. B. Yu, G. Q. Lo, and D. L. Kwong, "Cascade wide-angle Y-junction 1 x 16 optical power splitter based on silicon wire waveguides on silicon-on-insulator," Opt. Express **16**(26), 21456–21461 (2008).
26. P. B. Johnson, and R. W. Christy, "Optical constants of the Noble metals," Phys. Rev. B **6**(12), 4370–4379 (1972).
27. S. A. Maier, Plasmonics: Fundamentals and Applications (Springer, New York, 2007).

1. Introduction

Plasmonic waveguides have attracted much attention due to the ability to confine light beyond the diffraction limit, therefore enabling nano-scale dimension of the waveguide which is compatible with that of CMOS electronic components [1–9]. Since plasmonics offers a way to transfer and process both photonic and electronic signals along the same plasmonic circuit, it is certainly desirable to combine the advantage of both photonics and electronics that can lead to high signal processing speed and easy realization of active components [10].

In the past years several three-dimensional structures for plasmonic waveguides have been reported to support highly localized fields, e.g. metal-insulator-metal [2–5,8,9] and V-grooves in metal [6,7]. However, such nano-scale optical waveguides are usually pretty lossy and consequently the propagation distance is at the scale of several micrometers. However, for the practical case, it is very essential to have a propagation distance as long as several hundreds micrometers [11–13]. Recently, a deep subwavelenth plasmonic laser has been demonstrated experimentally by using a CdS-MgF_2-Ag hybrid plasmonic waveguide [14]. One should also note that silicon photonics has become very attractive because of its fabrication compatibility to the standard CMOS microelectronics technology [15,16]. Therefore it is really interesting to develop a silicon-based hybrid plasmonic waveguide [12,13,17–20]. In [12], we have presented a Si-based hybrid plasmonic waveguide with a metal cap for nano-scale light confinement as well as a long propagation distance. However, to our knowledge, there have not been many reports yet about the fundamental design and analysis of using the hybrid plasmonic waveguides for power splitters, which are very important elements for optical data-communications and telecommunications [21–25]. In this paper, we present 1×2 50:50 power splitters based on Si hybrid plasmonic waveguides by using the structures of multimode interference as well as Y-branch. We also analyze the bandwidth and fabrication tolerance of both kinds of power splitters. Finally, the feasibility of performing variable power splitters and 1×N power splitters are also discussed.

#137029 - $15.00 USD Received 22 Oct 2010; revised 24 Nov 2010; accepted 21 Dec 2010; published 6 Jan 2011

2. Design and analysis

Figure 1 (a) shows the schematic configuration of the Si hybrid plasmonic waveguide. A thin SiO_2 layer is sandwiched between a silicon-on-insulator (SOI) rib and a metal cladding. Considering the quasi-TM polarization, the field is enhanced at the thin low-index SiO_2 region due to the boundary condition of the electric field, which is similar to the horizontal slot waveguide. Here, we choose the geometrical dimensions as follows: h_m = 100 nm, h_{SiO2} = 10 nm, h_{Si_rib} = 200 nm and h_{Si} = 300 nm. We consider the wavelength λ = 1550 nm and the corresponding refractive indices for all the involved materials are n_{SiO2} = 1.445, n_{Si} = 3.455, and n_{metal} =0.1453 + 11.3587i (Ag), respectively. The complex refractive index of silver is from the measured result given by Johnson and Christy [26]. For the cap metal, one could use other metal materials, e.g., gold, which is very popular and more stable than silver. On the other hand, the conductivity of gold is not as good as silver and consequently the loss of the hybrid plasmonic waveguide with gold is more lossy. Figure 1(b) shows the calculated field distribution for the major component $E_y(x, y)$ of the quasi-TM fundamental mode when w=100 nm. For this calculation, we use a finite-element-method (FEM) mode solver (COMSOL). It can be seen that the optical field is highly confined in the 10 nm-thick SiO_2 layer. The propagation length of this hybrid plasmonic waveguide is about 70 μm, which provides a better compromise between the loss and the confinement than many plasmonic waveguides [2–9]. In the practical case, the optical waveguide usually contains some impurities introduced during the fabrication and thus becomes more lossy, which will limit the propagation distance in some degree. Some experimental results for this type Si hybrid plasmonic waveguide have also been demonstrated in Ref [19]. It has shown that the propagation length is up to about 40 μm, which was smaller than the calculated propagation length.

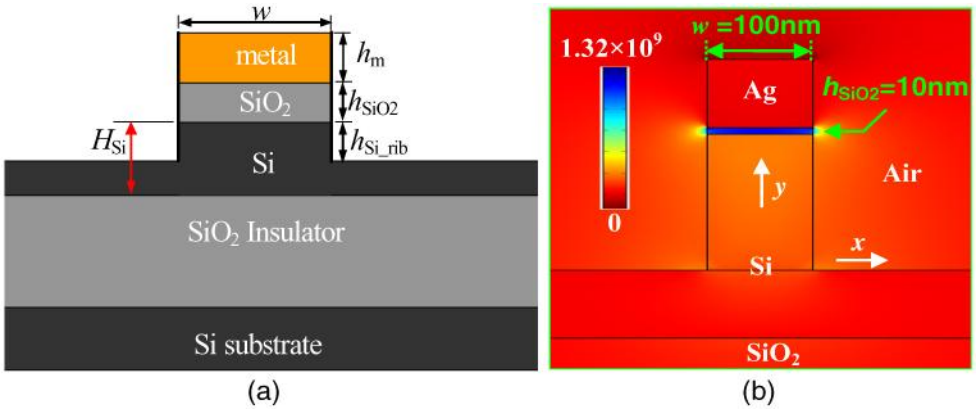

Fig. 1. (a) The cross section of the present hybrid plasmonic waveguide with a metal cap on a silicon-on-insulator rib with a thin SiO_2 interlayer; (b) the calculated field distribution for the major component $E_y(x, y)$ of the quasi-TM fundamental mode of the hybrid plasmonic waveguide.

Firstly we give an analysis for the multimode interference in a multimode hybrid plasmonic waveguide by using the FEM mode-solver and three-dimensional finite-difference time-domain (3D-FDTD) method (RSOFT). Figure 2 shows the real part of the effective indices and the propagation lengths for the fundamental and higher-order hybrid plasmonic modes as the width of the multimode waveguide increases. The cases of h_{SiO2}=5 nm, 10 nm, and 20 nm are considered here. One can see that when the width of the multimode waveguide is larger than 400 nm, the first higher-order mode of the hybrid plasmonic waveguide appears. There are more than five modes excited in the multimode waveguide when the width is larger than 1400 nm. Furthermore, when the h_{SiO2} decreases from 20 nm to 5 nm, the real part of effective index becomes larger, which means a higher index contrast laterally and consequently a more compact MMI device; however, the propagation length decreases

#137029 - $15.00 USD Received 22 Oct 2010; revised 24 Nov 2010; accepted 21 Dec 2010; published 6 Jan 2011

quickly due to a higher field confinement of the plasmonic waveguide. After balancing the propagation length, the field confinement, and the size of the MMI section, we choose h_{SiO2} = 10 nm in this paper. If no specially indicated, we choose h_m = 100 nm, h_{Si_rib} = 200 nm and H_{Si} = 300 nm in the rest of the designs and analysis.

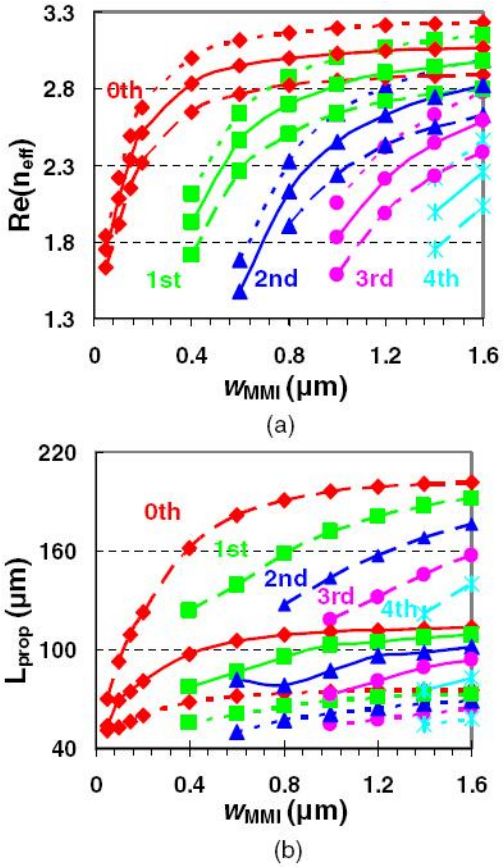

Fig. 2. (a) The real part of the effective index and (b) the propagation length for different order hybrid plasmonic modes (colored lines) as a function of the width of the multimode waveguide increase. The dotted line, solid line and dash line represent hSiO2 = 5 nm, 10 nm and 20 nm, respectively.

For a 1×2 power splitter, a 100 nm-wide singlemode plasmonic waveguide is used to launch the light into the multimode waveguide symmetrically. The width of the multimode waveguide is large enough to support higher-order modes. Since the symmetrically launched multimode waveguide cannot excite the first mode (odd mode) [21], the multimode waveguide should support the fundamental mode and the second order mode (even mode) for the case of a 1×2 MMI power splitter. Here, the width of the multimode waveguide is chosen to be w_{MMI}=650 nm to support these two modes (as shown in the right inset of Fig. 3 shown below). In order to reduce the coupling loss due to the mode mismatch, the input and output widths of the single mode waveguides are chosen to be tapered up to 200 nm with a 500 nm-long taper. Figure 3 shows the 3D-FDTD simulation result of the designed 1×2 MMI, when the length of the multimode waveguide L_{MMI}=530 nm. The grid sizes for the FDTD simulation are chosen as Δx = 25 nm, Δy = 2 nm, and Δz = 25 nm in order to obtain an accurate simulation for the light propagation. The transmission of this 1 × 2 MMI power splitter is about 91%. Here the transmission is defined as $(P_1 + P_2) / P_0$, where P_0, P_1 and P_2 are the input power, the output power from port #1 and port #2, respectively. The loss is mainly due to the intrinsic loss of the plasmonic waveguides, and the reflection at the interface between

#137029 - $15.00 USD Received 22 Oct 2010; revised 24 Nov 2010; accepted 21 Dec 2010; published 6 Jan 2011

the MMI section and the output waveguides. The upper inset of Fig. 3 shows the power distribution at the 10 nm-thick SiO_2 layer of the output waveguides.

Because of the fabrication errors of the E-beam lithography technology, the actual width of the MMI section might deviate from the design value (w_{MMI} = 650 nm). Figure 4(a) shows the simulation result for the transmission of the designed 1×2 MMI power splitter when there is a width deviation. From Fig. 4(a), it can be seen that the designed 1×2 50:50 MMI power splitter has a very large tolerance for the width. The transmission almost keeps around 91% when the width w_{MMI} has a deviation of ±50 nm. In Fig. 4(b), the wavelength dependence on the designed MMI coupler is shown. At the near-infrared wavelength regime, the dispersion of Ag can be represented by the Drude model [27]. By fitting the experimental data, one has the plasma frequency $\omega_p = 1.387 \times 10^{16}$ rad/s and collision frequency $\gamma = 3.087 \times 10^{13}$ rad/s. From Fig. 4(b), one sees that the transmission of the MMI power splitter is more than 80% in a wide wavelength range (from 1.25 μm to 1.7 μm). When the wavelength deviates from 1.55 μm, the transmission of the MMI power splitter decreases, because the multimode interference self-imaging position shifts in these cases.

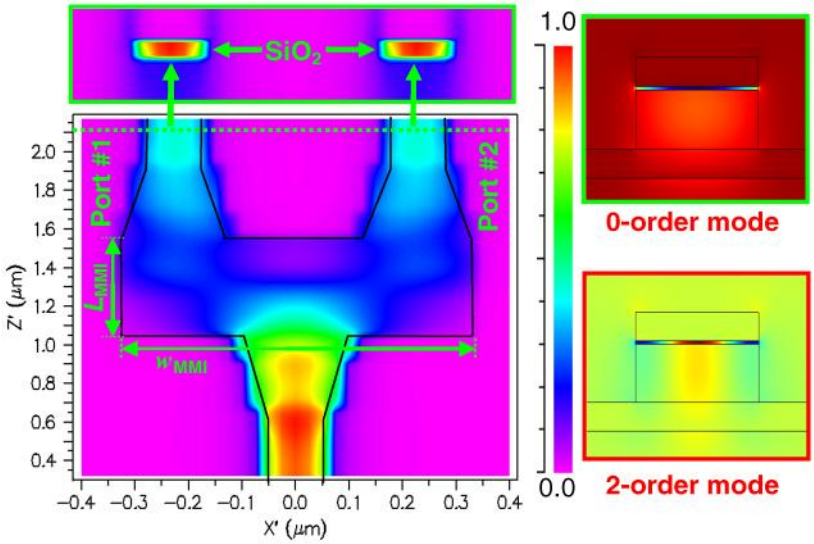

Fig. 3. Power propagation in the 1×2 50:50 MMI power splitter based on the multimode hybrid plasmonic waveguide with w_{MMI} = 650 nm and L_{MMI} = 530 nm. The right insets show the fundamental and second order modes of the MMI section; the upper inset shows the output power distribution at the 10 nm-thick SiO_2 layer.

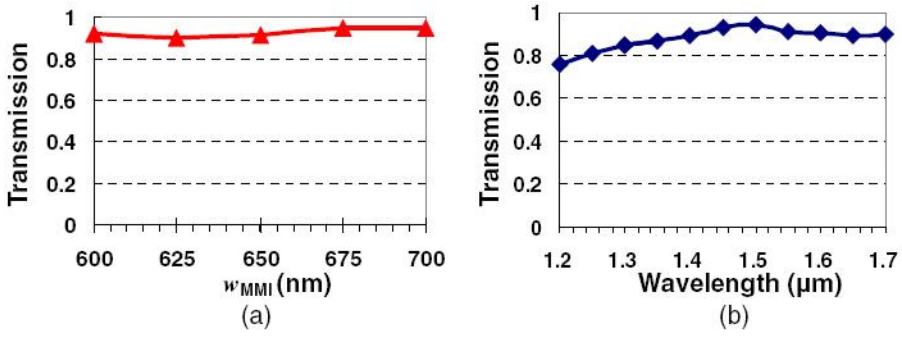

Fig. 4. Transmission of the 1×2 50:50 MMI power splitter as a function of (a) the width of the MMI (L_{MMI} = 530 nm) and (b) wavelength (L_{MMI} = 530 nm and w_{MMI} = 650 nm).

#137029 - $15.00 USD Received 22 Oct 2010; revised 24 Nov 2010; accepted 21 Dec 2010; published 6 Jan 2011

It is well known that a 50:50 power splitter is one of the most important fundamental elements for optical telecommunications and interconnects. On the other hand, variable power splitters that can tune the power splitting ratio are also very important for many applications. For example, in order to achieve a microring resonator with a high-Q factor and a high extinction ratio, a quite small coupling between the resonator and the input straight waveguide is needed. In this case, a 2×2 variable power splitter is the essential element as the coupler for the microring resonator. Here, we present a 2×2 variable power splitter by using the principle of two-mode interference (TMI), which was used to realize a silicon polarization splitter in Ref [23]. The TMI structure operates very similarly to the directional coupler while it is less sensitive to the dimension variations. The TMI coupler can be regarded as a directional coupler with zero-gap actually. Therefore, the light propagation in the multimode waveguide is similar to that in a directional coupler. Thus, variable power splitting ratio can be obtained by choosing the MMI length carefully. As Fig. 2 shows, when the width of the multimode waveguide is around 400 nm, only the two lowest order modes (the fundamental mode and the first order mode) can be supported. Here we choose the width 450 nm. In this case, S-bend waveguides are usually used to make two output waveguides separated enough in order to avoid the crosstalk between them. Here, we choose a 0.9μm-long S-bend with a radius of 0.75 μm (see detailed analyses in Fig. 6 (a)). In order to minimize the device footprint (as well as the loss), we introduce asymmetrical access waveguides by using a straight waveguide and a S-bend, respectively, as shown in the inset of Fig. 5(a). In this way, the two access waveguides are almost decoupled. Figure 5(a) shows the transmission and the power splitting ratio of the port #1 and port #2. The simulated light propagation in the TMI coupler is also shown in this figure. One can see that the power splitting ratio could be adjusted from 97.1%:2.9% to 1.7%:98.3% as the TMI length increases from 0.8 μm to 1.7 μm. The overall footprint is about 0.8 μm ×2.6 μm. The transmission of the variable power splitter is around 0.5, which is mainly due to the bend loss and intrinsic loss of hybrid plasmonic waveguides. Though the increase of insertion loss and device footprint is due to S-bends waveguides, here the S-bends waveguides are inevitable to avoid the across talk in the two-mode interference coupler. When the TMI length is chosen to be 1.7 μm, the power splitting ratio is about 1.7%:98.3%. Such a power splitter/coupler could be used for the applications when a small part of power needs to be tapped out, e.g., power monitors. Figure 5(b) shows the wavelength dependence of this 1.7%:98.3% power splitter. One can see that it has a large bandwidth of 1.4 μm-1.7 μm. In this range the transmission is about 0.5 and the power splitting ratio is about 2%:98%.

#137029 - $15.00 USD Received 22 Oct 2010; revised 24 Nov 2010; accepted 21 Dec 2010; published 6 Jan 2011

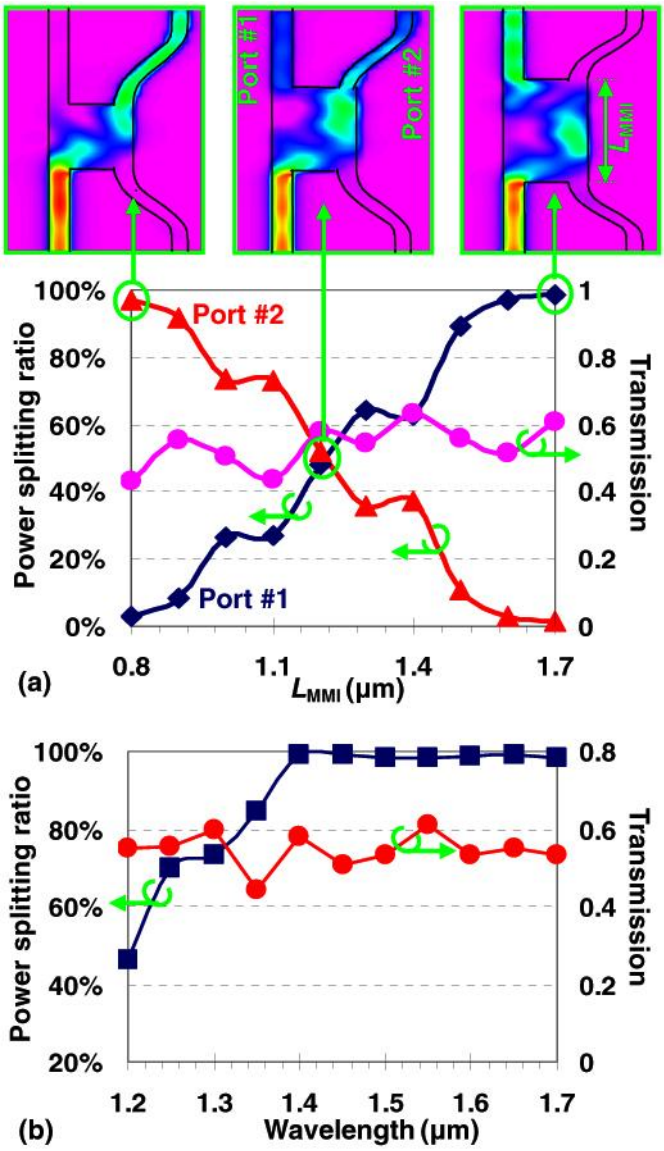

Fig. 5. (a) The transmission and power splitting ratio of the 2×2 MMI power splitter as the MMI length L_{MMI} changes (w_{MMI} = 450 nm). The upper insets show the power propagation for the case of L_{MMI}=0.8μm, 1.2μm, and 1.7μm; (b) the transmission and power splitting ratio of the designed 1.7%:98.3% 2×2 MMI power splitter with L_{MMI}=1.7μm as a function of wavelength.

Comparing with pure dielectric waveguides, the hybrid plasmonic waveguide still has a relatively large loss. Consequently the self-imaging quality becomes deteriorated especially when the MMI width is large, which is needed for a 1×N power splitter with large port number. In this aspect, a cascaded Y-branch is a potential choice better than an MMI coupler because of its easy design and large fabrication tolerance. In the flowing sections, the Y-branch power splitters based on the hybrid plasmonic waveguides are analyzed to make a comparison with the MMI coupler.

In order to obtain a 50:50 power splitter, a symmetric Y-branch consisting of two 100 nm-wide S-bends with a separation of D=600 nm is considered, as shown in Fig. 6(b). In this case, the coupling length of the output waveguides is about 43μm, which is large enough to

#137029 - $15.00 USD Received 22 Oct 2010; revised 24 Nov 2010; accepted 21 Dec 2010; published 6 Jan 2011

avoid the crosstalk for micro-scale plasmonic circuits. Two S-bends are directly connected to the straight waveguide, and the overlapping region of these two S-bends can be considered as a taper, splitting the power of the straight waveguide into two branches. For the design of the Y-branch, the length of the S-bend, $L_{\text{S-bend}}$, needs to be long enough to guarantee a low leakage loss (i.e., the bending radius should be large enough) and to avoid any mode distortion. However, a short S-bend is preferred to have a compact size and low loss due to the intrinsic absorption loss of metal. Therefore, there is a trade-off when choosing the s-bend length. Figure 6(a) shows the transmission of the 1×2 Y-branch power splitter as the length of the S-bend increases (or the radius increases). One can see that there is a relatively low transmission when $L_{\text{S-bend}}$ <0.7 μm or $L_{\text{S-bend}}$ >3 μm. This is because of the total loss is contributed by the bending leakage loss and intrinsic absorption loss of metal in the same time. And the highest transmission is about 92%, which is achieved when $L_{\text{S-bend}}$ is about 1.9 μm. Furthermore, in order to reduce the size, here we choose $L_{\text{S-bend}}$=0.9 μm (the corresponding radius is 0.75 μm), and the transmission of the Y-branch power splitter is about 90%. Figure 6(b) shows the power propagation in the designed 1×2 Y-branch 50:50 power splitter with $L_{\text{S-bend}}$ =0.9 μm and D = 600 nm. Such a design has a wide angle between these two S-bends, which makes it easily realized by using the electron beam lithography technology.

Figure 7(a) and 7(b) shows the simulated transmission of the 1×2 50:50 Y-branch power splitter as the waveguide width and the wavelength deviate from the designed values, respectively. From these figures, one sees that the 1×2 50:50 Y-branch power splitter has a large width fabrication tolerance (−50 nm~50 nm), and a large bandwidth of 1.2 μm-1.7 μm, in which range the transmission is about 90%.

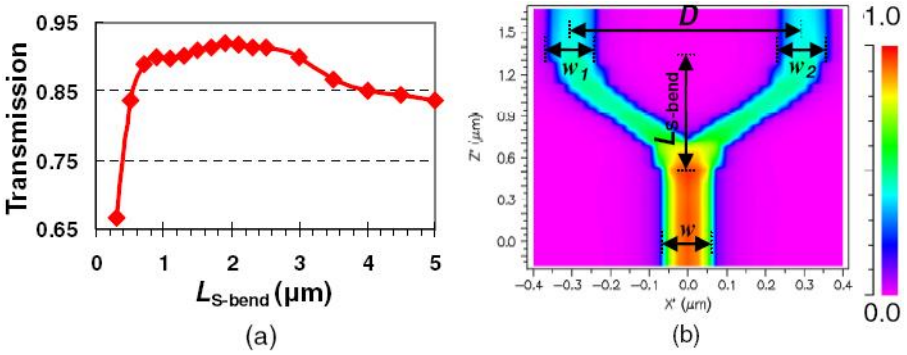

Fig. 6. (a) The transmission of the 1×2 Y-branch power splitter as the S-bend length increases; (b) The power propagation in the designed 1×2 50:50 Y-branch power splitter with $L_{\text{S-bend}}$ = 0.9 μm and D = 600 nm.

#137029 - $15.00 USD Received 22 Oct 2010; revised 24 Nov 2010; accepted 21 Dec 2010; published 6 Jan 2011

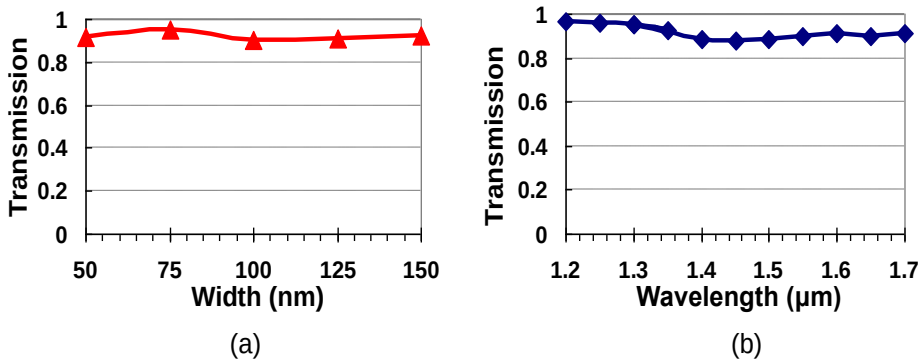

Fig. 7. The transmission of the designed 1×2 50:50Y-branch power splitter with $L_{S\text{-}bend}$ = 0.9 μm and D = 600 nm as a function of (a) the waveguide width (w=w_1=w_2), and (b) the wavelength.

It is well known that an asymmetric Y-branch with different S-bend width can be used for a variable Y-branch power splitter for dielectric waveguides. Here we present a simple variable power splitter based on the hybrid plasmonic waveguides by using an asymmetric Y-branch. In our design, one of the arms of the Y-branch is fixed to be w_2=200 nm while the width of the other arm, w_1, varies from 50 nm to 200 nm. Correspondingly the calculated power splitter ratio varies in the range from 84%:16% to 16%:84% (as shown in Fig. 8 (a)). This variable range is a bit larger than that of the common dielectric variable Y-branch power splitter [24]. Comparing to the variable MMI power splitter, the total transmission of the variable Y-branch power splitter is almost unchanged when the width w_1 changes. Additionally, the power splitter ratio can be tuned in a larger range by shifting the center position of the narrow S-bend with w_1 = 50 nm.

Finally, we cascaded two stages of Y-branches to obtain a 1×4 power splitter, as shown in Fig. 8 (b). In order to reduce the crosstalk of the output waveguides, a relative large Y-branch with $L_{S\text{-}bend1}$ =1.2 μm and D_1 = 1200 nm (the radius is also 0.75 μm) is used for the first stage. For the second stage, two smaller Y-branches with $L_{S\text{-}bend2}$ =0.9 μm and D_2 = 600 nm are used. Between the two stages, a 0.5 μm-long straight waveguide is used to connect them. Figure 8 (b) shows the power propagation in the 1×4 Y-branch power splitter based on the two stages of cascaded Y-branches. The inset shows the power distributions at the four output waveguides. One can see that the total transmission of the 1×4 power splitter is about 83%, and the power distributions in the four output waveguides (from left to right) are 25.6%, 24.3%, 25.6%, and 24.5%, respectively. The device footprint of the designed 1×4 power splitter is about 1.9 μm×2.6 μm. Compared to the 1×4 power splitter based on silicon waveguides [25], the device footprint of the present 1×4 power splitter based on Si hybrid plasmonic waveguides is about 1/1200 smaller. On the other hand, due to the intrinsic loss of the hybrid plasmonic waveguide, the loss of the present 1×4 power splitter is a little higher than the pure dielectric one.

#137029 - $15.00 USD Received 22 Oct 2010; revised 24 Nov 2010; accepted 21 Dec 2010; published 6 Jan 2011

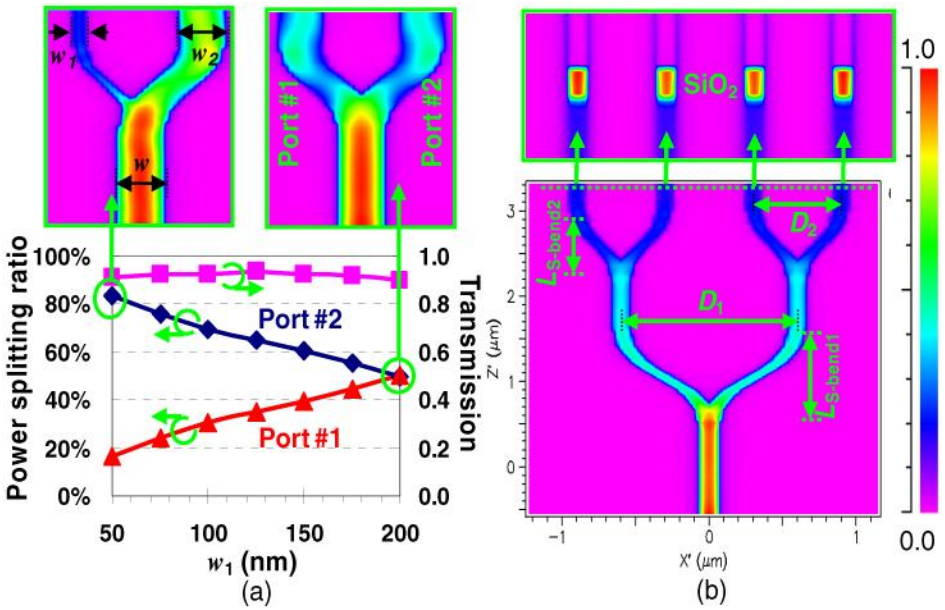

Fig. 8. (a) The power splitting ratio of the 1×2 Y-branch power splitter as the S-bend width w_1 increases (w_2=200 nm). The upper insets in Fig. 8.(a) show the power transmission for the case of w_1=50 nm and 200 nm; (b) the power propagation in the 1×4 Y-branch power splitter with $L_{S\text{-bend1}}$ = 1.2 μm and D_1 = 1200 nm, $L_{S\text{-bend2}}$ = 0.9 μm and D_2 = 600 nm. The upper inset in Fig. 8(b) shows the output power distribution at the 10 nm-thick SiO_2 layer.

3. Conclusion

In this paper, we have given a detailed discussion of various power splitters based on the Si hybrid plasmonic waveguides by using an MMI structure as well as Y-branch. The optimized MMI power splitter and Y-branch power splitter have the sizes of 650 nm×530 nm and 900 nm×600 nm, respectively. The fabrication tolerance of the waveguide width is as large as ±50 nm and the bandwidth is over 500 nm. The designed 1×2 50:50 power splitters have high power transmission of around 90%. The asymmetrical power splitter has been also designed by using a 2×2 two-mode interference structure and an asymmetric Y-branch. Their power splitting ratios are potentially adjustable from 97.1%:2.9% to 1.7%:98.3% and from 84%:16% to 16%:84%, respectively. The large adjustable power splitting ratio of the 2×2 two-mode coupler makes it become a good option to be the coupler for high-Q microring resonators with a high extinction ratio. Furthermore, since the 1×2 50:50Y-branch power splitter has an ultracompact size and relative low loss, it can be helpful to achieve a 1×N power splitter (through cascading) for data-communications and telecommunications. One should note that the hybrid plasmonic waveguide has a relatively long propagation distance (~70 μm) while it is still lossy. For the sake of long-distance optical interconnect, one can integrate the hybrid plasmonic devices with pure Si nanowires and the corresponding coupling loss is about 1.5dB [20].

Acknowledgments

This project was partially supported by Zhejiang Provincial Natural Science Foundation (No.R1080193), the National Nature Science Foundation of China (No. 61077040), and the "111" Project (No. B07031).

#137029 - $15.00 USD Received 22 Oct 2010; revised 24 Nov 2010; accepted 21 Dec 2010; published 6 Jan 2011